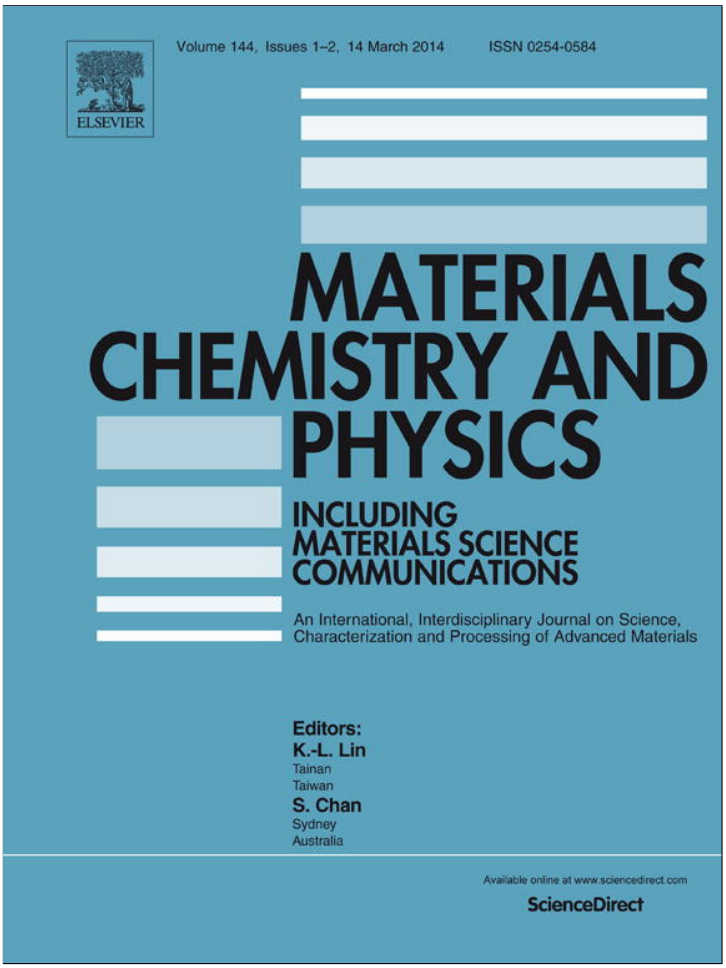

Materials Chemistry and Physics 144 (2014) 206–211

Contents lists available at ScienceDirect

Materials Chemistry and Physics

journal homepage: www.elsevier.com/locate/matchemphys

Scaling analysis of PM–FM phase transition in $Nd_{0.5}Sr_{0.25}Ca_{0.25}MnO_3$ based on magnetic entropy change

Jiyu Fan [a], Weichun Zhang [a,*], Xiyuan Zhang [a], Lei Zhang [b], Yuheng Zhang [b,c]

[a] Department of Applied Physics, Nanjing University of Aeronautics and Astronautics, Nanjing 210016, China
[b] High Magnetic Field Laboratory, Chinese Academy of Sciences, Hefei 230031, China
[c] Hefei National Laboratory for Physical Sciences at the Microscale, University of Science and Technology of China, Hefei 230026, China

HIGHLIGHTS

- The nature of the second-order ferromagnetic phase transition can be clarified by the magnetic entropy change scaling.
- The high magnetic field can drive the whole phase transition from first- to second-order phase transition.
- This method is effective to distinguish different order ferromagnetic phase transitions.

ARTICLE INFO

Article history:
Received 11 August 2013
Received in revised form
3 December 2013
Accepted 31 December 2013

Keywords:
Magnetic materials
Solidification
Magnetic properties
Phase transitions

ABSTRACT

The dependence of magnetization M on temperature T and the applied magnetic field H were measured for the half-doping manganite $Nd_{0.5}Sr_{0.25}Ca_{0.25}MnO_3$. The $M(T)$ curve exhibits that a paramagnetic (PM) –ferromagnetic (FM) phase transition occurs around 174 K. The PM–FM phase transition is considered to be a second-order phase transition due to the absence of hysteresis on its heating and cooling $M(T)$ curves. Moreover, the second-order phase transition can be testified with the positive slope in Arrott plots. However, the scaling analysis of magnetic entropy change exhibits that $\Delta S_M(T)$ curves do not collapse into a single universal curve, indicating that the observed PM–FM phase transition is not an authentic second-order phase transition. Due to the appearance of short-range FM coupling in PM region, the PM–FM phase transition at 225 K > T > 188 K is a first-order phase transition. The second-order phase transition only occurs at T < 188 K. When the magnetic field is increased above 1.5 T, the first-order phase transition can be converted into the second-order phase transition. The results shows that the magnetic entropy change scaling is an effective method to determine the nature of the PM–FM phase transition.

1. Introduction

Magnetic refrigeration is becoming a promising technology to replace the conventional vapor compression-based refrigeration due to its high efficiency and environmental friendliness. This technology is based on the magnetocaloric effect (MCE) which is the reversible temperature change of a magnetic material upon the application or removal of magnetic field [1]. As a material is magnetized by the magnetic field, the entropy associated with the magnetic degree of freedom (S_M) decreases. Under adiabatic conditions, the reduction of magnetic entropy change (ΔS_M) is accompanied by an increase of the lattice entropy, and the temperature of the material rises. Conversely, when the magnetic field is removed the magnetic spins become randomize, increasing the magnetic entropy change and lowering the lattice entropy and decreasing temperature of the material. The warming and cooling process in response to the external magnetic field is called MCE. In order to build a magnetic refrigerator operating with higher efficiency, it requires magnetic refrigerant exhibiting larger MCE. The magnetic entropy change (ΔS_M) can be calculated from the equation of $\Delta S_M = \int_0^H (\partial M/\partial T)_H dH$. Thus, the MCE is expected to be maximum around Curie temperature as magnetic materials exhibit an abrupt change of magnetization in paramagnetic (PM) to ferromagnetic (FM) phase transition.

According to the different orders of PM–FM phase transition, the magnetocaloric materials can be classified into the first-order

* Corresponding author. Tel.: +86 25 52075728; fax: +86 25 83336919.
E-mail address: weichun@nuaa.edu.cn (W. Zhang).

0254-0584/$ – see front matter
http://dx.doi.org/10.1016/j.matchemphys.2013.12.048

materials and second-order ones. Generally, the materials undergoing the first-order phase transition show a very large MCE, like $Gd_5Si_2Ge_2$ [2], Ni_2MnGa [3], $MnFeP_{0.45}As_{0.55}$ [4]. However, the first order material has some obvious shortcomings in the practical application. First of all, the presence of thermal/magnetic hysteresis is not conducive for actual refrigeration cycles. Secondly, the first-order phase transition exhibits a very narrower ΔS_M peak and hence its refrigerant capacity is very small (refrigerant capacity, which is a measure of the amount of heat transferred between the hot and cold reservoirs, is an important parameter to characterize MCE) [5]. In contrast, for the second-order materials, although they only show a moderate magnetic entropy change, the lack of thermal/magnetic hysteresis and a broader ΔS_M peak (large refrigerant capacity) exhibits a great advantage in practical magnetic refrigeration. Therefore, the application of the second-order materials has been paid a more attention in the recent years [6]. The colossal magnetoresistance manganites with the formula $R_{1-x}A_xMnO_3$ (R = rare earth element, A = divalent alkaline earth element) also display MCE and a comprehensive summary of the MCE in manganites can be found in the review by Phan and Yu [7]. These manganites display either a first-order or a second-order PM–FM phase transition [8–11]. Usually, Arrott plots (M^2 vs. H/M curve) are established to study the nature of PM–FM phase transition. According to the criterion proposed by Banerjee [12], the order of phase transition can be determined from the slope of lines in Arrott plot. The positive slope corresponds to the second-order transition while the negative slope corresponds to the first-order transition. However, Bonilla et al. have recently found that this criterion is not very clear to determine the nature of PM–FM phase transition in some materials such as $DyCo_2$ [13]. They proposed a new criterion to distinguish the order of PM–FM phase transition depending on the phenomenological model introduced by Franco et al. [14]. This method is based on the existence of "universal master curve" for the ΔS_M under different applied magnetic fields when the magnetic phase transition is of the second-order type in nature, where the universal behavior is ascribed to the collapse of the points in the ΔS_M curves for equivalent states. However, for the first-order material, there is not a "universal master curve" because the systematical state in the hysteretic region is inequivalent. In this case, the application of the universal scaling on the ΔS_M curve will lead to a breakdown rather than a collapse. More recently, being a representative first-order sample of bulk $La_{0.7}Ca_{0.3}MnO_3$, Lampen et al. utilized this MCE-based universal curve method to study the impact of reduced dimensionality on the phase order [15]. They found that the reduction in dimensionality in film and the controllable particle size in nanocrystalline can change the previous first-order into second-order phase transition. In this paper, we will apply this method to study and check the nature of PM–FM phase transition of the half-doping manganite $Nd_{0.5}Sr_{0.25}Ca_{0.25}MnO_3$, which displays a totally different phase transition as that in some usual half-doping manganites.

2. Experiment

Polycrystalline sample $Na_{0.5}Sr_{0.25}Ca_{0.25}MnO_3$ was prepared by the conventional solid-state reaction method with high-purity Nd_2O_3, $SrCO_3$, $CaCO_3$, and MnO_2 as the starting materials. The mixture was preheated in air at 900 °C for 24 h. Afterward the powder was ground and heated at 1200 °C for 30 h. Finally, it was reground, pressed into pellets and sintered for another 40 h at 1350 °C, and was cooled down to room temperature with the furnace. The structure and phase purity has been checked by X-ray powder diffraction. The sample is a single phase and exhibits the orthorhombic structure. The magnetization M measurement was performed using a conventional Quantum Design MPMS system under 0.01 T magnetic field over the temperature range of 5–300 K. The isothermal magnetization curves were measured with a maximum sweep field of 3.0 T at different temperatures.

3. Results and discussion

The physical properties of the hole-doped manganite $R_{1-x}A_xMnO_3$ are decided by the different doping concentration x. As $x = 0.5$, like $La(Pr,Nd)_{0.5}Ca_{0.5}MnO_3$, it generally behaves as a periodic arrangement of Mn^{3+} and Mn^{4+} ions at Mn-site sublattice, which is called charge ordering phase. As the presence of charge ordering phase, a thermal hysteresis occurs in the heating and cooling measurements of magnetization and resistivity because the charge disordering-charge ordering transition is the first-order phase transition [16,17]. For the present $Nd_{0.5}Sr_{0.25}Ca_{0.25}MnO_3$ system, as a half-doped material, it should exhibit a hysteresis on its heating and cooling $M(T)$ curves. As shown in Fig. 1(b), however, the heating curve overlaps the cooling one at the whole temperature range. By contrast, two adjacent samples, $Nd_{0.5}Sr_{0.2}Ca_{0.3}MnO_3$ and $Nd_{0.5}Sr_{0.3}Ca_{0.2}MnO_3$, their hysteresis can be clearly observed from Fig. 1(a) and (c). The absence of hysteresis implies the lack of charge ordering transition in $Nd_{0.5}Sr_{0.25}Ca_{0.25}MnO_3$. The reason has been clarified in our previous report with the A-site cation disorder induced by the size mismatch between Sr^{2+} and Ca^{2+} ions [18]. Therefore, the PM–FM phase transition observed in Fig. 1(b) can be referred to be second-order phase transition. However, as mentioned in the introduction section, the nature of the above PM–FM phase transition need to be further clarified. The inset of Fig. 1(b) presents the inverse magnetization as a function of temperature. The solid line is the fitting result by using Curie–Weiss law $\chi = C/(T-\theta)$, where $C = N_A\mu_B^2P_{eff}^2/3k_B$ is the Curie constant, N_A is Avogadro constant, μ_B is the Bohr magneton, $P_{eff} = gS(S+1)$ is the effective magnetic moment, $g = 2$ is the gyromagnetic ratio and S is

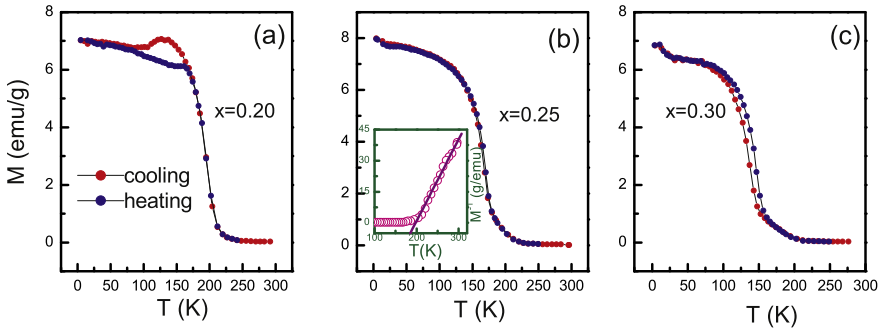

Fig. 1. Temperature dependence of magnetization measured at 100 Oe with cooling and heating cycle for $Nd_{0.5}Sr_{0.5-x}Ca_xMnO_3$.

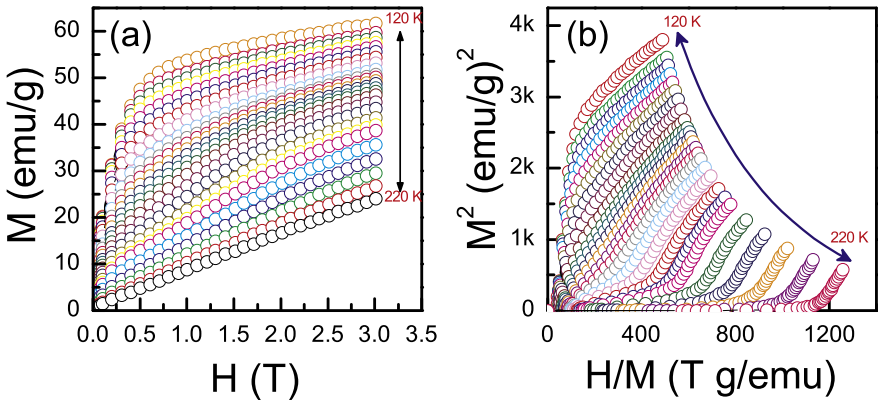

Fig. 2. (a) Magnetic isotherms (M vs. H) at various temperatures in the field range up to 3.0 T, (b) Arrott plots (M^2 vs. H/M) obtained from the magnetic isotherms.

the magnetic spin, k_B is Boltzmann constant, θ is paramagnetic Weiss temperature. From the fitting Curie constant C, the effective magnetic moment was calculated to be $P_{eff} = 6.45\mu_B$, which is larger than the theoretical value $4.38\mu_B$ (Here, the theoretical magnetic moment of Mn^{3+} and Mn^{4+} ions are taken as 4.9 and $3.8\mu_B$, respectively.) The discrepancy between experiment and theory implies that some short-range FM couplings might have developed in the PM region and contribute the additional magnetic moments. This phenomena are generally recalled as "magnetic phase separation" and have been extensively reported in manganites [19–22].

Arrott plots are generally established to study the nature of a PM–FM phase transition, based on the isothermal magnetization data. Fig. 2(a) shows the isothermal magnetization data measured for $Nd_{0.5}Sr_{0.25}Ca_{0.25}MnO_3$ around its Curie temperature 174 K. To establish Arrott plot, the isothermal magnetization data were converted into M^2 vs. H/M relationship, namely, Arrott plots as plotted in Fig. 2(b). Obviously, all the curves show a positive slope indicating that the current PM–FM phase transition in Fig. 1(b) is of a second order one. However, the order of PM–FM phase transition determined only from Arrott plot is not very accurate as suggest by Bonilla and Franco [13,14]. According to the method suggested by Bonilla et al., the rescaled ΔS_M vs. T curves under different magnetic fields collapse into a single curve only for the second-order materials. Therefore, the order of phase transition in the present system will be further clarified by utilizing this method.

The main idea of this method is to select two points on each ΔS_M vs. T curves. One (T_{r1}) is below T_{peak} and the other (T_{r2}) is above T_{peak}. These two points must satisfy the relation $\Delta S_M(T_{r1}) = \Delta S_M(T_{r2}) = k\Delta S_M^{peak}(T_{peak})$, where ΔS_M^{peak} is the maximum value of the selected ΔS_M vs. T curves and k is the relative value of the entropy changes at two reference temperatures T_{r1} and T_{r2}. Generally, the selection of k value is arbitrary but k value is always between 0 and 1. In fact, theoretical investigation has demonstrated that it is unnecessary to use two reference temperature but just alone for a single magnetic phase material [23]. However, in the case of the coexistence of multiple magnetic phases and complex PM–FM phase transition, the selection of two reference temperatures is necessary. Given the half-doped manganites $Nd_{0.5}Sr_{0.25}Ca_{0.25}MnO_3$, the additional magnetic phase transition can not be completely excluded. Therefore, two reference temperatures are used here and the temperature axis is rescaled as:

$$\theta = \begin{cases} \theta_- = \left(T_{peak} - T\right) \Big/ \left(T_{r1} - T_{peak}\right), T < T_{peak} \\ \theta_+ = \left(T - T_{peak}\right) \Big/ \left(T_{r2} - T_{peak}\right), T > T_{peak} \end{cases} \quad (1)$$

In order to testify the collapse or breakdown of the entropy change curve on different applied fields, we first calculate the entropy change at different temperatures by using $|\Delta S_M| = \sum(M_{i+1} - M_i/T_{i+1} - T_i)\Delta H_i$, where M_i and M_{i+1} are the experimental data of the magnetization at T_i and T_{i+1}, respectively, under the magnetic field H_i. Based on the isothermal magnetization values in Fig. 2(a), Fig. 3(a) gives the calculated ΔS_M as a function of temperature under different fields. All $\Delta S_M(T)$ curves display a unimodal shape. The maximum entropy change occurs at T_{peak} on each $\Delta S_M(T)$ curves. It is noticed that T_{peak} shows a slight field dependence and moves to a high temperature. In principle, T_{peak} keeps a constant temperature only under the framework of mean-field model. However, for $Nd_{0.5}Sr_{0.25}Ca_{0.25}MnO_3$, its critical exponents β and γ have been reported to be 0.386 and 1.174, respectively

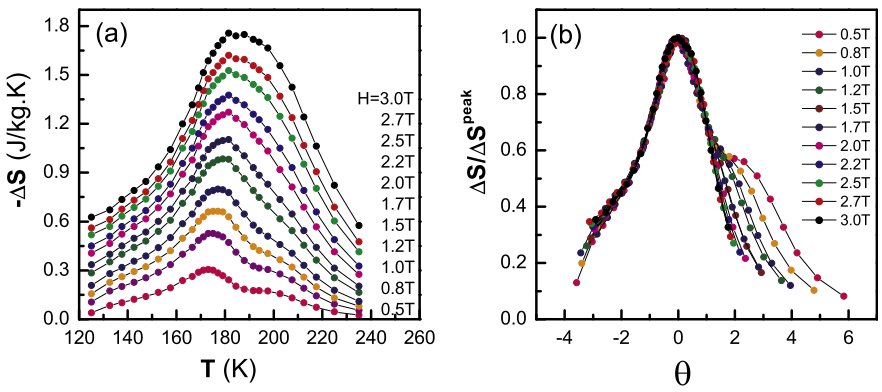

Fig. 3. (a) Temperature dependence of magnetic entropy change under different applied magnetic fields for $Nd_{0.5}Sr_{0.25}Ca_{0.25}MnO_3$, (b) normalized magnetic entropy change dependence of the rescaled temperatures.

[24]. Therefore, its critical behavior of PM–FM phase transition can be described with 3D-Heisenberg model. This model is generally applied in a magnetic system with short-range interaction [25,26]. As previously mentioned, the present sample is a phase separation system. In the PM region, the PM and FM coexistence inevitably cause an inhomogeneous state. The high magnetic field is favorable for FM phase to grow up quickly. Consequently, the PM–FM phase transition will naturally be driven to higher temperature region, consistent with the observation of a slight dependence of increasing T_{peak} with magnetic field in Fig. 3(a). Fig. 3(b) shows the ΔS_M normalized to ΔS_M^{peak} as a function of the rescaled temperature θ (using Eq. (1)). Even though the k value is arbitrary but a medium value is generally expected to yield a high-quality universal curve. Here, we choose the $k = 0.7$ to construct the "universal master curve". As shown in Fig. 3(b), all the ΔS_M vs. T curves do not collapse into a single curve but display an obvious breakdown. However, the breakdown only occurs at $\theta > 1$ and $H < 1.2$ T regions. This results contains two potential meanings: (i) The $\theta > 1$ corresponds to the temperature axis of $T > 180$ K region, indicating that the second-order PM–FM phase transition only stars in the temperature blow 180 K. (ii) The temperature of second-order phase transition can be driven to higher temperature of $T > 200$ K as the magnetic field is applied above 1.2 T. This result clearly indicates that there is a first-order PM–FM phase transition at $T > 180$ K, but which can be changed into second-order phase transition under higher magnetic field. Recently, the magnetic field-driven phase transition from first-order to second order has been testified in another manganite $La_{0.8}Ca_{0.2}MnO_3$ [27].

Fig. 4(a) shows the deviation of temperature (breakdown from universal curve) at different magnetic fields. Obviously, with the increase of the magnetic field, the degree of deviation significantly reduces. As the magnetic field reaches 1.5 T, the temperature of deviation can be ignored, indicating that the high magnetic field enlarges the temperature range of second-order phase transition. In order to declare this variation clearly, Fig. 4(b) shows the differential magnetization vs. temperature curve under 100 Oe magnetic field. From it, one can find that the part signed with yellow circle is significantly different from its front and back of the changes. It starts at 225 K and ends at 188 K. During this temperature range, the sample yields an initial PM–FM phase transition but it is a first-order phase transition, consistent with the breakdown in Fig. 3(b). After that, the system enters into next stage which is the second-order phase transition. In the present sample, the ratio of Mn^{3+}:Mn^{4+} is fixed to 1. The size mismatch between Sr^{2+} and Ca^{2+} ions causes A-site cation disorder, which induced the random distribution of Mn^{3+} and Mn^{4+} ions. Therefore, it is possible to form some short-range FM states above 188 K. These short-range FM phases are so weak that they do not form a stable long-range PM–FM phase. However, with the help of a certain high magnetic field, these short-range FM phases are easy to enlarge and transform into a state FM structure. Thus, a discontinuous phase transition is changed into a continuous phase transition. Fig. 4(c) shows the magnetization vs. temperature under different fields. With the increase of magnetic field, a small bump occurred at 180 K $< T <$ 220 K slowly disappears, indicating the process of increasing FM region and decreasing inhomogeneity. Therefore, in Fig. 3(b), all $\Delta S_M(T)$ vs. T curves collapse into a single curve only as the magnetic field is above 1.5 T.

In addition, we also investigated the variations of T_{r1}, T_{r2} and T_{peak} induced by applying magnetic field. Their variations are displayed in Fig. 4(d). Except T_{r1}, T_{r2} and T_{peak} show some different variations as the applied field is blow and above 1.5 T. For T_{peak}, it always increases at $H < 1.5$ T while remains the same temperature at $H > 1.5$ T. This variation implies that the applied magnetic field drives the PM–FM phase transition to high temperature region. As $H = 1.5$ T, the localized inhomogeneous phase has been suppressed and all PM–FM phase transitions change into second-order phase transition. Therefore, the T_{peak} does not increase as the rise of applied magnetic field. Because T_{r1} is smaller than T_{peak}, the region of T_{r1} is in the FM state. On this occasion, the systemic PM–FM phase transition has been finished and the whole magnetic structure has become a complete FM state. The applying magnetic field

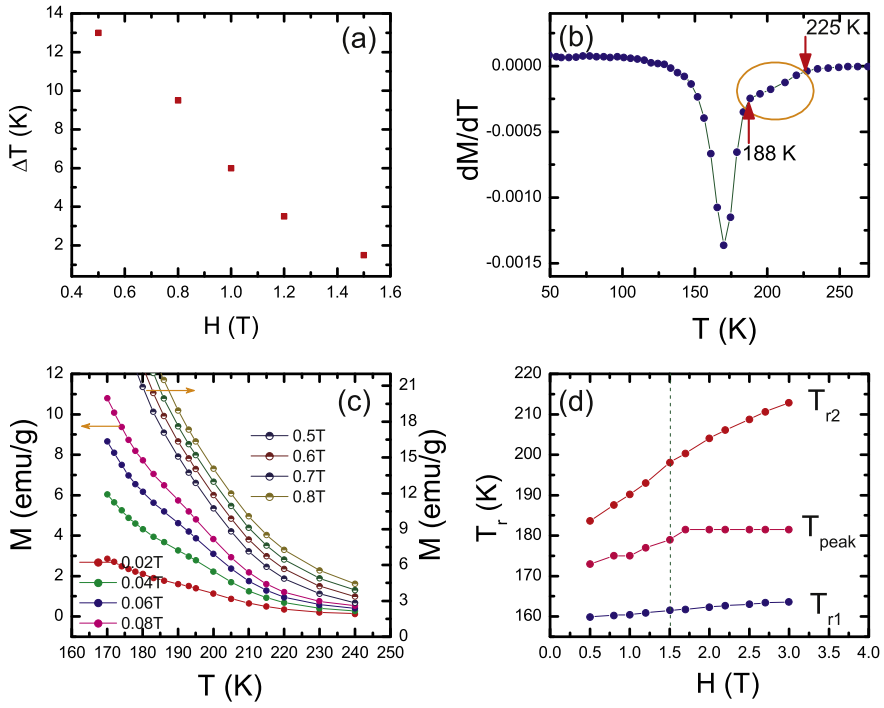

Fig. 4. (a) Deviation of temperature under different magnetic fields, (b) derivative of magnetization with respect to temperature (dM/dT), (c) temperature dependence of magnetization measured at different magnetic fields, (d) magnetic field dependence of T_{r1}, T_{r2} and T_{peak}.

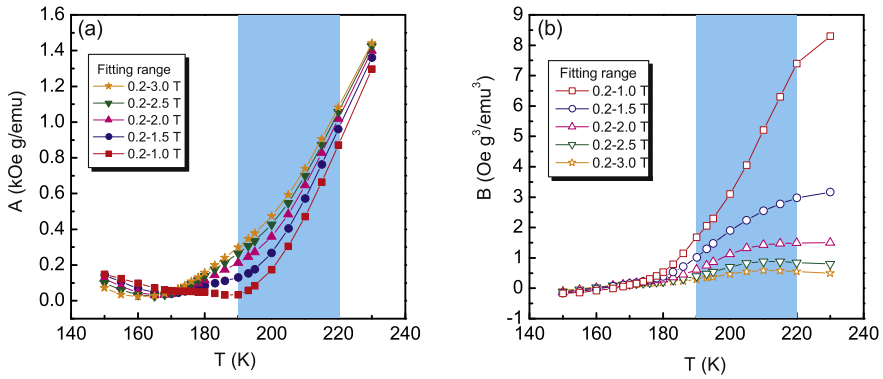

Fig. 5. The temperature dependence of parameters A and B obtained by fitting Landau–Lifshitz equation in different magnetic field ranges.

has no obvious effect on the variation of T_{r1}. On the contrary, T_{r2} is larger than T_{peak}. Its region belongs to the PM region or PM–FM phase transitional region. As discussed earlier, the external magnetic field can force the growth of local FM state and decrease inhomogeneity. Therefore, T_{r2} shows a continuous increase until the magnetic field is applied to 3.0 T. However, the variation of T_{r2} at $H < 1.5$ T is larger than that at $H > 1.5$ T, implying that the systemic inhomogeneity of the PM state has been signally decreased as the magnetic field is above 1.5 T. We noticed that, for a single second-order system, the variations of T_{r1} and T_{r2} exhibited a symmetric broadening, namely, an increase of T_{r2} and a decrease of T_{r1} with the increase of applied magnetic field. For example, for the spinel selenide $CuCr_2Se_4$ which shows a clear low field MCE [28], both T_{r1} and T_{r2} present a linear relation with the applied magnetic field $H^{1/\Delta}$, where $\Delta = \beta + \gamma$. However, the results of Fig. 4(d) indicate that this relation fails to apply in the present system. We can conjecture that the influence of local magnetic inhomogeneous state is not completely ruled out even though the high magnetic field can drive the whole phase transition to become a second-order phase transition.

In order to further verify the magnetic field driven-phase transition from first- to second-order, we used the Landau–Lifshitz theory to analysis the above PM–FM phase transition in the different applying magnetic field. According to Landau–Lifshitz theory, the equation of state can be expressed as

$$H = A(T)M + B(T)M^3 + C(T)M^5 + \ldots \quad (2)$$

For a general magnetic system, we only need to consider the front two terms and determine the order of phase transition from the sign of $B(T)$. However, Zhang et al. recently found that the higher order terms can't be ignored as a system just lies in the middle of first- and second-order phase transition [27]. Therefore, we used the above equation to fit the $M(H)$ curves with different magnetic field ranges. Fig. 5 shows the fitting parameters of $A(T)$ and $B(T)$. The temperature corresponding to the zero value of parameter A is consistent with the Curie temperature T_C [29]. From Fig. 5(a), one can find that, except for the curve with the fitting range of 0.2–1.0 T, the minimum A values on the other curves are almost close to zero as $T \sim 172$ K, basically consistent with $T_C = 174$ K determined from $M(T)$ curve. However, the minimum A value appeared around 190 K on the curve with maximum fitting range of 1.0 T significantly deviate from the rule, indicating that the systemical inhomogeneity at PM region was effectively suppressed as the magnetic field was applied above 1.5 T. Moreover, in Fig. 5(b), one can find that the B value under the different magnetic fields displays a more conspicuous variations. At temperature range of 190 K $\leq T \leq$ 220 K, the B value, which is related to the elastic and the magnetoelastic terms of free energy [29,30], dramatically reduce at the lower fitting magnetic field but it shows a slightly change at the higher field. Under the maximum fitting field range of 0.2–3.0 T, the B value almost remains a constant. This phenomenon reveals that the magnetoelastic property is dependence on temperature at low magnetic field while independence on temperature at high magnetic field. In the current system, the range of 190 K $\leq T \leq$ 220 K belongs to PM region. The low magnetic field is insufficient to eliminate inhomogeneity so that the B value changes sharply. On the contrary, the high magnetic field favors for the formation of long-range FM state and drives the phase transition from first- to second-order. Therefore, in Fig. 3(b), the universal master curve only be observed for all the temperature range as the applying magnetic field is above 1.5 T.

4. Conclusion

In summary, we have studied the PM–FM phase transition in the half-doped manganites $Nd_{0.5}Sr_{0.25}Ca_{0.25}MnO_3$ by using the scaling analysis of magnetic entropy change. Due to the appearance of the local magnetic inhomogeneity in the system, the sample first undergoes a first-order phase transition and then enters into a second-order phase transition. When the magnetic field is increased enough, the whole PM–FM phase transition completely converts into a second-order phase transition. Therefore, a first-order phase transition crossover a second-order phase transition can be driven with the high magnetic field. The present work also stresses the importance of the scaling analysis of magnetic entropy change in elucidating the nature of magnetic phase transition.

Acknowledgment

This work was supported by NUAA Fundamental Research Funds (grant no. NS2013079).

References

[1] E. Warburg, Annu. Phys. Chem. 13 (1881) 141.
[2] V.K. Pecharsky, K.A. Gschneidner, Phys. Rev. Lett. 78 (1997) 4494.
[3] F.X. Hu, B.G. Shen, J.R. Sun, Appl. Phys. Lett. 76 (2000) 3460.
[4] O. Tegus, E. Brück, K.H.J. Buschow, F.R. de Boer, Nature(London) 415 (2002) 150.
[5] V. Franco, J.S. Blazquez, B. Ingale, A. Conde, Annu. Rev. Mater. Res. 42 (2012) 305.
[6] V. Franco, A. Conde, Int. J. Refrig. 33 (2010) 465.
[7] M.H. Phan, S.C. Yu, J. Magn. Magn. Mater. 308 (2007) 325.
[8] K. Ghosh, C.J. Lobb, R.L. Greene, S.G. Karabashev, D.A. Shulyatev, A.A. Arsenov, Y. Mukovskii, Phys. Rev. Lett. 81 (1998) 4740.
[9] P. Novák, M. Maryško, M.M. Savosta, A.N. Ulyanov, Phys. Rev. B 60 (1999) 6655.

[10] T. Sarkar, A.K. Raychaudhuri, A.K. Bera, S.M. Yusuf, New J. Phys. 12 (2010) 123026.
[11] M.H. Phan, V. Franco, N.S. Bingham, H. Srikanth, N.H. Hur, J. Alloys Compd. 508 (2010) 238.
[12] S.K. Banerjee, Phys. Lett. 12 (1964) 16.
[13] C.M. Bonilla, J. Herrero-Albillos, F. Bartolome, L.M. Garcia, M. Parra-Borderias, V. Franco, Phys. Rev. B 81 (2010) 224424.
[14] V. Franco, J.S. Blazquez, A. Conde, Appl. Phys. Lett. 89 (2006) 222512.
[15] P. Lampen, N.S. Bingham, M.H. Phan, H. Kim, M. Osofsky, A. Piqué, T.L. Phan, S.C. Yu, H. Srikanth, Appl. Phys. Lett. 102 (2013) 062414.
[16] R. Mahendiran, B. Raveau, M. Hervieu, C. Michel, A. Maignan, Phys. Rev. B 64 (2001) 064424.
[17] F. Rivadulla, E. Winkler, J.-S. Zhou, J.B. Goodenough, Phys. Rev. B 66 (2002) 174432.
[18] Jiyu Fan, Langsheng Ling, Li Pi, Yang Wang, Yue Ying, Yuheng Zhang, J. Appl. Phys. 100 (2006) 053902.
[19] M.H. Phan, M.B. Morales, N.S. Bingham, H. Srikanth, C.L. Zhang, S.W. Cheong, Phys. Rev. B 81 (2010) 094413.
[20] M. Quintero, J. Sacanell, L. Ghivelder, A.M. Gomes, A.G. Leyva, F. Parisi, Appl. Phys. Lett. 97 (2010) 121916.
[21] J. Deisenhofer, D. Braak, H.-A. Krug von Nidda, J. Hemberger, R.M. Eremina, V.A. Ivanshin, A.M. Balbashov, G. Jug, A. Loidl, T. Kimura, Y. Tokura, Phys. Rev. Lett. 95 (2005) 257202.
[22] A.L. Lima Sharma, P.A. Sharma, S.K. McCall, S.-B. Kim, S.-W. Cheong, Appl. Phys. Lett. 95 (2009) 092506.
[23] V. Franco, A. Conde, J.M. Romero-Enrique, J.S. Blazquez, J. Phys. Condens. Matter 20 (2008) 285207.
[24] Jiyu Fan, Bo Hong, Lei Zhang, Yangguang Shi, Wei Tong, Langsheng Ling, Li Pi, Yuheng Zhang, J. Magn. Magn. Mater. 322 (2010) 3692.
[25] S.N. Kaul, J. Magn. Magn. Mater. 53 (1985) 5.
[26] Jiyu Fan, Langsheng Ling, Bo Hong, Lei Zhang, Li Pi, Yuheng Zhang, Phys. Rev. B 81 (2010) 144426.
[27] P. Zhang, P. Lampen, T.L. Phan, S.C. Yu, T.D. Thanh, N.H. Dan, V.D. Lam, H. Srikanth, M.H. Phan, J. Magn. Magn. Mater. 348 (2013) 146.
[28] Lei Zhang, Jiyu Fan, Wei Tong, Langsheng Ling, Li Pi, Yuheng Zhang, Physica B 407 (2012) 3543.
[29] V.A. Amaral, J.S. Amaral, J. Magn. Magn. Mater. 272 (2004) 2104.
[30] J.S. Amaral, M.S. Reis, V.A. Amaral, T.M. Mendonca, J.P. Araúji, M.A. Sá, P.B. Tvares, J.M. Vieira, J. Magn. Magn. Mater. 290 (2005) 686.